

RD-A165 956

INTERACTION OF MOVING SHOCK WITH THIN STATIONARY

1/1

THERMAL LAYER(U) AEROSPACE CORP EL SEGUNDO CA

AEROPHYSICS LAB H MIRELS 20 FEB 86 TR-0086(6785)-2

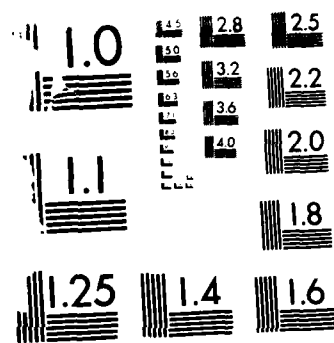
UNCLASSIFIED

SD-TR-86-08 F04701-85-C-0086

F/G 18/3

NL





MICROCOPY RESOLUTION TEST CHART
 (ANSI/ISO 1967-2)

AD-A165 956

Interaction of Moving Shock
with Thin Stationary Thermal Layer

HAROLD MIRELS
Aerophysics Laboratory
Laboratory Operations
The Aerospace Corporation
El Segundo, Calif. 90245

20 February 1986

DTIC
SELECTE
MAR 25 1986
S D

APPROVED FOR PUBLIC RELEASE;
DISTRIBUTION UNLIMITED

Prepared for
DEFENSE NUCLEAR AGENCY
Washington, DC 20305

FILE COPY

SPACE DIVISION
AIR FORCE SYSTEMS COMMAND
Los Angeles Air Force Station
P.O. Box 92960, Worldway Postal Center
Los Angeles, Calif. 90009-2960

040

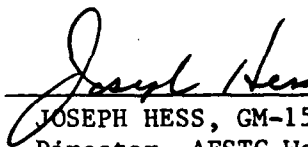
This report was submitted by The Aerospace Corporation, El Segundo, CA 90245, under Contract No. F04701-85-C-0086 with the Space Division, P.O. Box 92960, Worldway Postal Center, Los Angeles, CA 90009-2960. It was reviewed and approved for The Aerospace Corporation by W. P. Thompson, Director, Aerophysics Laboratory. Major Douglas Joslyn, Space Division/YOC, was the project officer for the Mission-Oriented Investigation and Experimentation (MOIE) Program.

This report has been reviewed by the Public Affairs Office (PAS) and is releasable to the National Technical Information Service (NTIS). At NTIS, it will be available to the general public, including foreign nationals.

This technical report has been reviewed and is approved for publication. Publication of this report does not constitute Air Force approval of the report's findings or conclusions. It is published only for the exchange and stimulation of ideas.



DOUGLAS JOSLYN, Major, USAF
MOIE Project Officer
SD/YOC



JOSEPH HESS, GM-15
Director, AFSTC West Coast Office
AFSTC/WCO OL-AB

UNCLASSIFIED

SECURITY CLASSIFICATION OF THIS PAGE (When Data Entered)

REPORT DOCUMENTATION PAGE		READ INSTRUCTIONS BEFORE COMPLETING FORM
1. REPORT NUMBER SD-TR-86-08	2. GOVT ACCESSION NO. ADA 165 956	3. RECIPIENT'S CATALOG NUMBER
4. TITLE (and Subtitle) INTERACTION OF MOVING SHOCK WITH THIN STATIONARY THERMAL LAYER		5. TYPE OF REPORT & PERIOD COVERED
		6. PERFORMING ORG. REPORT NUMBER TR-0086(6785)-2
7. AUTHOR(s) Harold Mirels		8. CONTRACT OR GRANT NUMBER(s) F04701-85-C-0086
9. PERFORMING ORGANIZATION NAME AND ADDRESS The Aerospace Corporation El Segundo, Calif. 90245		10. PROGRAM ELEMENT, PROJECT, TASK AREA & WORK UNIT NUMBERS
11. CONTROLLING OFFICE NAME AND ADDRESS Defense Nuclear Agency Washington, DC 20305		12. REPORT DATE 20 February 1986
		13. NUMBER OF PAGES 26
14. MONITORING AGENCY NAME & ADDRESS (if different from Controlling Office) Space Division Los Angeles Air Force Station Los Angeles, Calif. 90009-2960		15. SECURITY CLASS. (of this report) Unclassified
		15a. DECLASSIFICATION/DOWNGRADING SCHEDULE
16. DISTRIBUTION STATEMENT (of this Report) Approved for public release; distribution unlimited.		
17. DISTRIBUTION STATEMENT (of the abstract entered in Block 20, if different from Report)		
18. SUPPLEMENTARY NOTES		
19. KEY WORDS (Continue on reverse side if necessary and identify by block number) Nuclear Blast Shock Wave Thermal Layer Thermal Precursor		
20. ABSTRACT (Continue on reverse side if necessary and identify by block number) An analytical model is presented for the interaction between a moving shock and a thin thermal layer of semi-infinite extent. The fluid is assumed to be inviscid and ideal. The model is based on flow field characteristics deduced from the detailed numerical code calculations of Schneyer and Wilkins (1984). Flow field properties of interest include the peak surface (stagnation) pressure at the base of the incident shock, the forward extent of the shock-induced precursor, and the surface pressure at the latter		

UNCLASSIFIED

SECURITY CLASSIFICATION OF THIS PAGE(When Data Entered)

19. KEY WORDS (Continued)

20. ABSTRACT (Continued)

location. Good agreement with Schneyer and Wilkins is obtained subject to appropriate choice of an arbitrary constant k introduced into the analytical model. Further validation of the model is needed. *found*

find

UNCLASSIFIED

SECURITY CLASSIFICATION OF THIS PAGE(When Data Entered)

CONTENTS

I.	INTRODUCTION.....	5
II.	THEORY.....	7
	A. Unseparated Flow Regime.....	10
	B. Separated Flow Regime.....	27
III.	DISCUSSION.....	27
IV.	CONCLUSION.....	29
	REFERENCES.....	31
	SYMBOLS.....	33



Accession For	
NTIS CRA&I	<input checked="" type="checkbox"/>
DTIC TAB	<input type="checkbox"/>
Unannounced	<input type="checkbox"/>
Justification	
By	
Distribution /	
Availability Codes	
Dist	Avail and/or Special
A-1	

FIGURES

1.	Initial Conditions in Laboratory Stationary Coordinate System.....	8
2.	Unseparated Steady Flow in Incident Shock Stationary Coordinate System.....	9
3.	Boundary Between Separated and Unseparated Flow Regimes.....	11
4a.	Numerical Results of Ref. 5 for Shock-Thermal Layer Interaction.....	12
4b.	Numerical Results of Ref. 5 for Shock-Thermal Layer Interaction.....	13
4c.	Numerical Results of Ref. 5 for Shock-Thermal Layer Interaction.....	14
5.	Schematic Representation of Shock-Thermal Interaction for Case of Separated Flow.....	15
6a.	Interface Trajectories Based on Numerical Solution of Ref. 5.....	16
6b.	Interface Trajectories Based on Numerical Solution of Ref. 5.....	17
7.	Boundary Conditions Near Interface x_1 in Incident Shock Stationary Coordinate System, $k \equiv \cos \theta$	22

I. INTRODUCTION

It is well known that radiation from a nuclear explosion can generate a thin layer of heated air adjacent to the ground.¹ The interaction of the nuclear blast wave with this thermal layer results in a precursor wave system, which affects dust cloud generation and the aerodynamic load on ground structures.¹ A general discussion of this interaction has been provided by Hess.² Experimental studies of the interaction of weak ($\bar{M}_g < 1.14$) moving shocks with thin thermal layers have been reported in Refs. 3 and 4.

Detailed numerical code calculations of the inviscid interaction between an incident shock and a thin thermal layer of semi-infinite streamwise extent have recently been reported.⁵ The present study is an attempt to deduce properties of the latter interaction by simple analytic methods and to compare with the numerical results of Ref. 5.

II. THEORY

Consider a normal shock wave moving over a thin thermal layer of semi-infinite extent and assume ideal gases. The initial flow field, in laboratory stationary coordinates, is illustrated in Fig. 1. For generality, the ratio of specific heats γ is allowed to differ in the thermal layer and in the external flow. After the initial transient, the interaction can be characterized as either unseparated or separated. These flows are steady and unsteady, respectively, in incident shock stationary coordinates. Both cases are considered herein. Flow velocity and Mach number are denoted by \bar{u} and \bar{M} , respectively, in the laboratory coordinate system (Fig. 1), and by u and M in the incident shock stationary coordinate system (Fig. 2). Note that $\bar{M}_s \equiv \bar{u}_s/a_1 = u_1/a_1 = M_1$.

A. UNSEPARATED FLOW REGIME

We consider unseparated steady flow in a shock stationary coordinate system (Fig. 2). The static pressure downstream of the incident shock is⁵

$$\frac{p_2}{p_1} = \frac{2\gamma_1 M_1^2 - (\gamma_1 - 1)}{\gamma_1 + 1} \quad (1)$$

The stagnation pressure in the downstream portion of the thermal layer is⁶

$$\frac{p_{5,t}}{p_4} = \left[1 + \left(\frac{\gamma_4 - 1}{2} \right) M_4^2 \right]^{\gamma_4/(\gamma_4 - 1)} \quad M_4 < 1 \quad (2a)$$

$$= \left[\left(\frac{\gamma_4 + 1}{2} \right) M_4^2 \right]^{\gamma_4/(\gamma_4 - 1)} \left[\frac{\gamma_4 + 1}{2\gamma_4 M_4^2 - (\gamma_4 - 1)} \right]^{1/(\gamma_4 - 1)} \quad M_4 > 1 \quad (2b)$$

As noted in Ref. 2, the interaction between the shock and thermal layer will remain unseparated and steady (in shock fixed coordinates) provided

$p_{5,t}/p_4 > p_2/p_1$. The flow becomes separated and unsteady when $p_{5,t}/p_4 <$

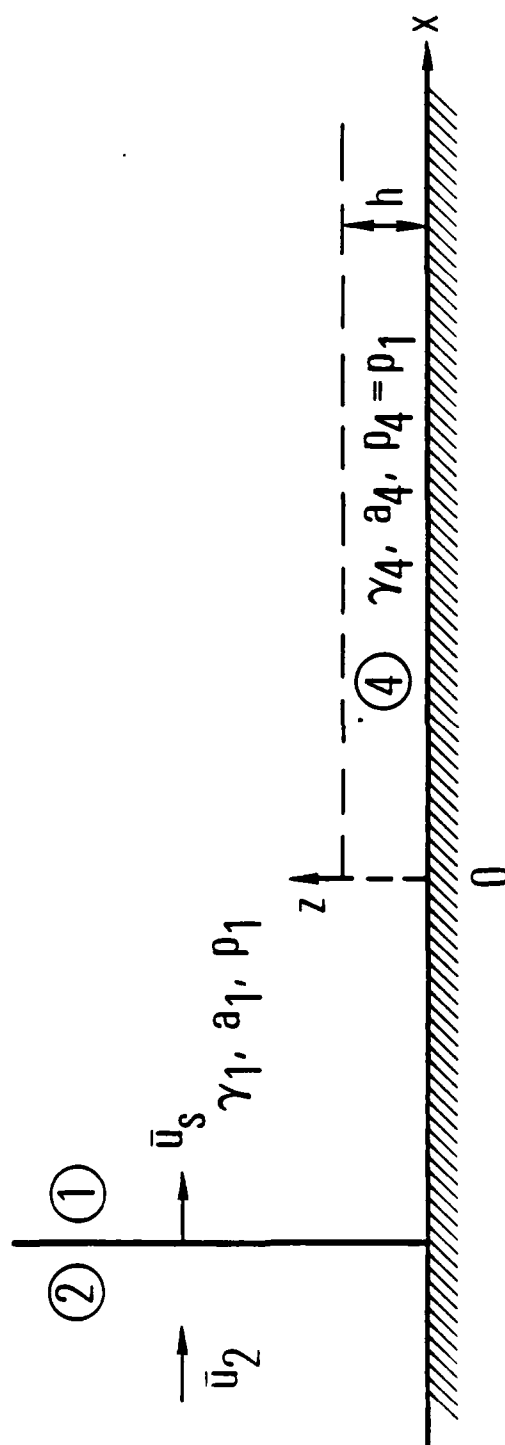


Fig. 1. Initial Conditions in Laboratory Stationary Coordinate System

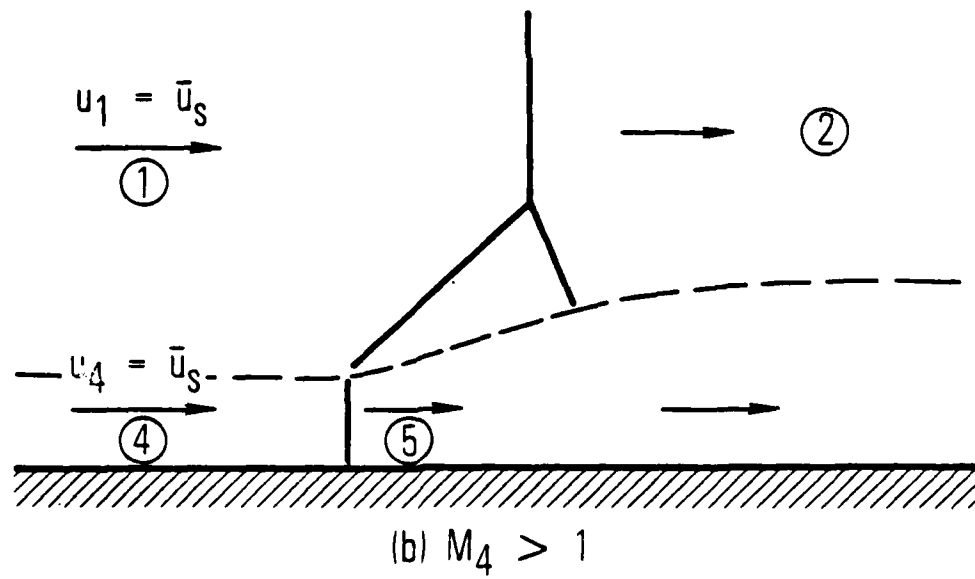
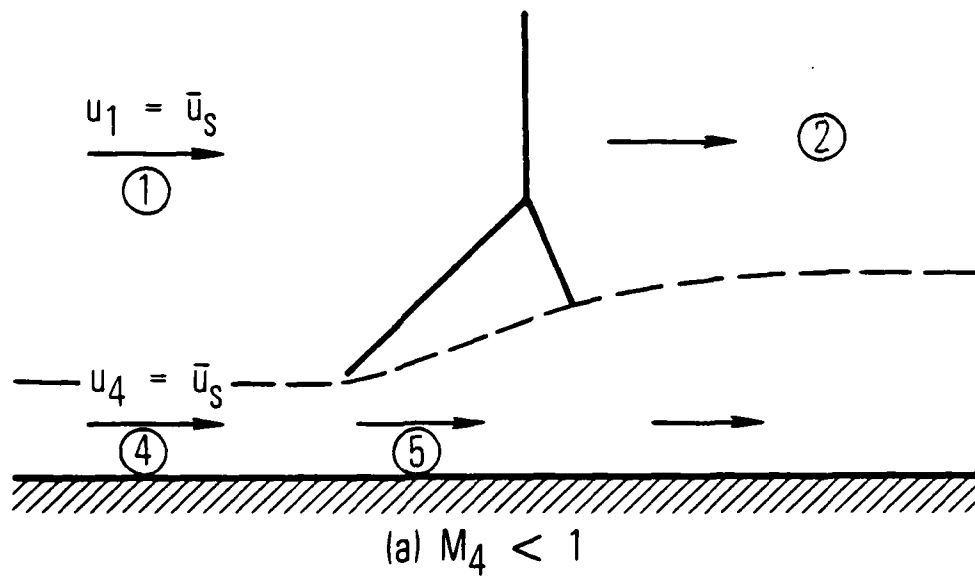


Fig. 2. Unseparated Steady Flow in Incident Shock Stationary Coordinate System

p_2/p_1 . The boundary between the separated and unseparated flow regimes is obtained by equating Eqs. 1 and 2 and noting $M_4 = (a_1/a_4)M_1$. The results are given in Fig. 3 and agree with similar results in Ref. 2. The unseparated flow regime occurs for values of a_4/a_1 and M_1 near one. Increased values of a_4/a_1 and/or M_1 lead to a separated flow, which is discussed in the next section.

B. SEPARATED FLOW REGIME

Numerical results from Ref. 5 and an analytic model are presented herein.

1. NUMERICAL RESULTS

Detailed numerical calculations of the interaction between an incident shock and a thermal layer have been presented in Ref. 5 for various incident shock Mach numbers \bar{M}_s and speed of sound ratios a_4/a_1 . Specific heat ratio values $\gamma_1 = 1.4$ and $\gamma_4 = 5/3$ (approximately) were assumed so that the interface between the fluid in regions 1 and 4 was well defined. Viscous effects were neglected.

Results from Ref. 5 are given in Table 1 and Fig. 4. Figs. 4(a) and 4(b) provide density contours at a fixed instant of time ($x_s = 20.1$ cm), and Fig. 4(c) provides the corresponding pressure distribution at three heights above the ground. Initial conditions were $\bar{M}_s = 2.61$ and $a_4/a_1 = 2.26$. The latter was termed Case II in Ref. 5. A schematic representation of the flow field, inferred from Fig. 4, is given in Fig. 5(a) using coordinates wherein the incident shock is stationary. Shock-heated gas originally from region 1 moves forward of the incident shock and separates the thermal layer gas flow from the wall. The interface between gas from region 1 and gas from region 4 is indicated by a dashed line in Fig. 5(a). The interface location at the wall is denoted x_i . The quantities x_{sp} , x_s , and x_{st} , in Fig. 5(a), denote the streamwise location of a stagnation point, the incident shock, and the leading edge of the normal shock in the thermal layer, respectively. The corresponding locations of these stations are included in Fig. 4. The variation of these locations, with time, deduced from the data reported in Ref. 5, are given in Fig. 6. The local slope of the curves in Fig. 6 define local velocity. These results indicate that, after an initial transient, the

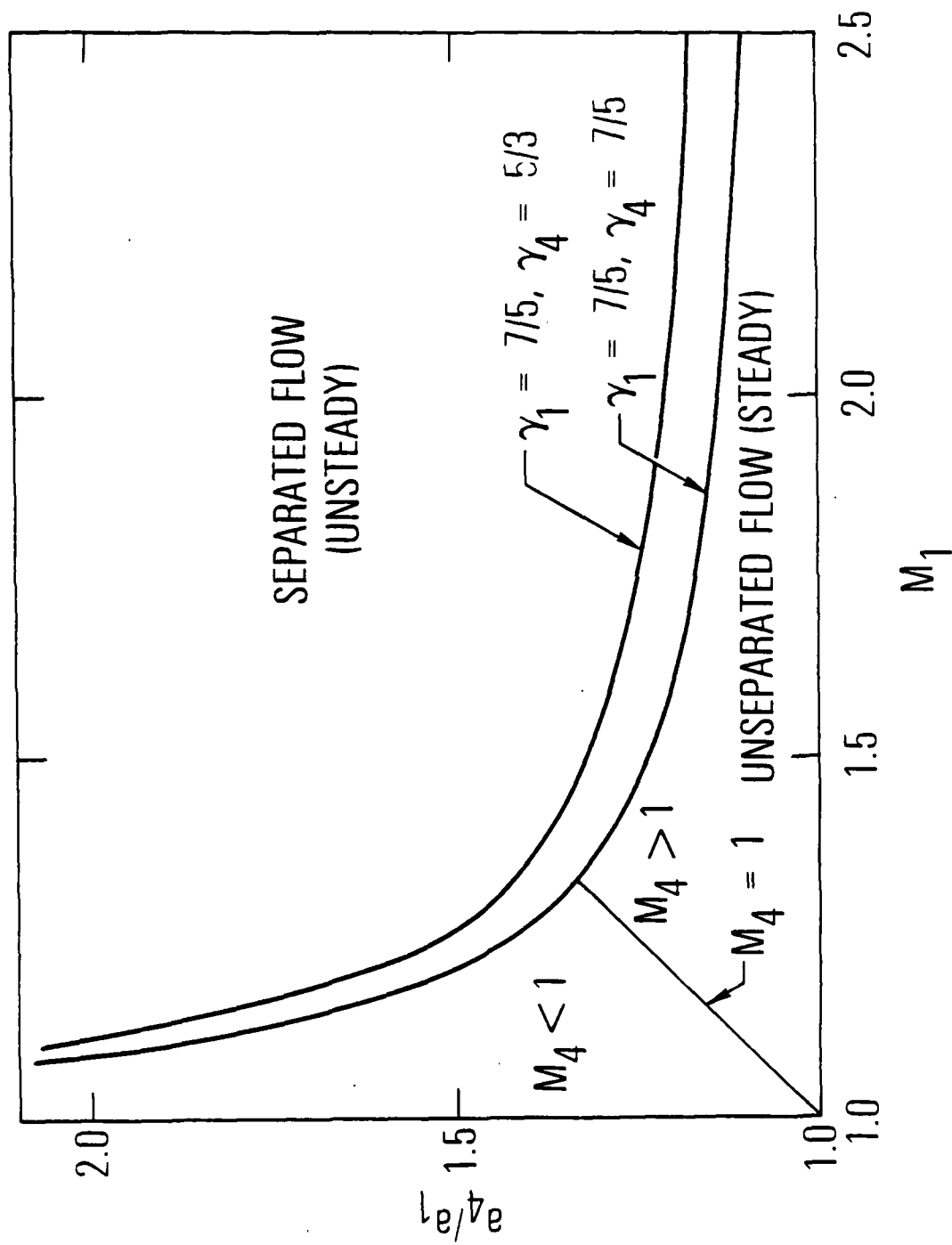


Fig. 3. Boundary Between Separated and Unseparated Flow Regimes

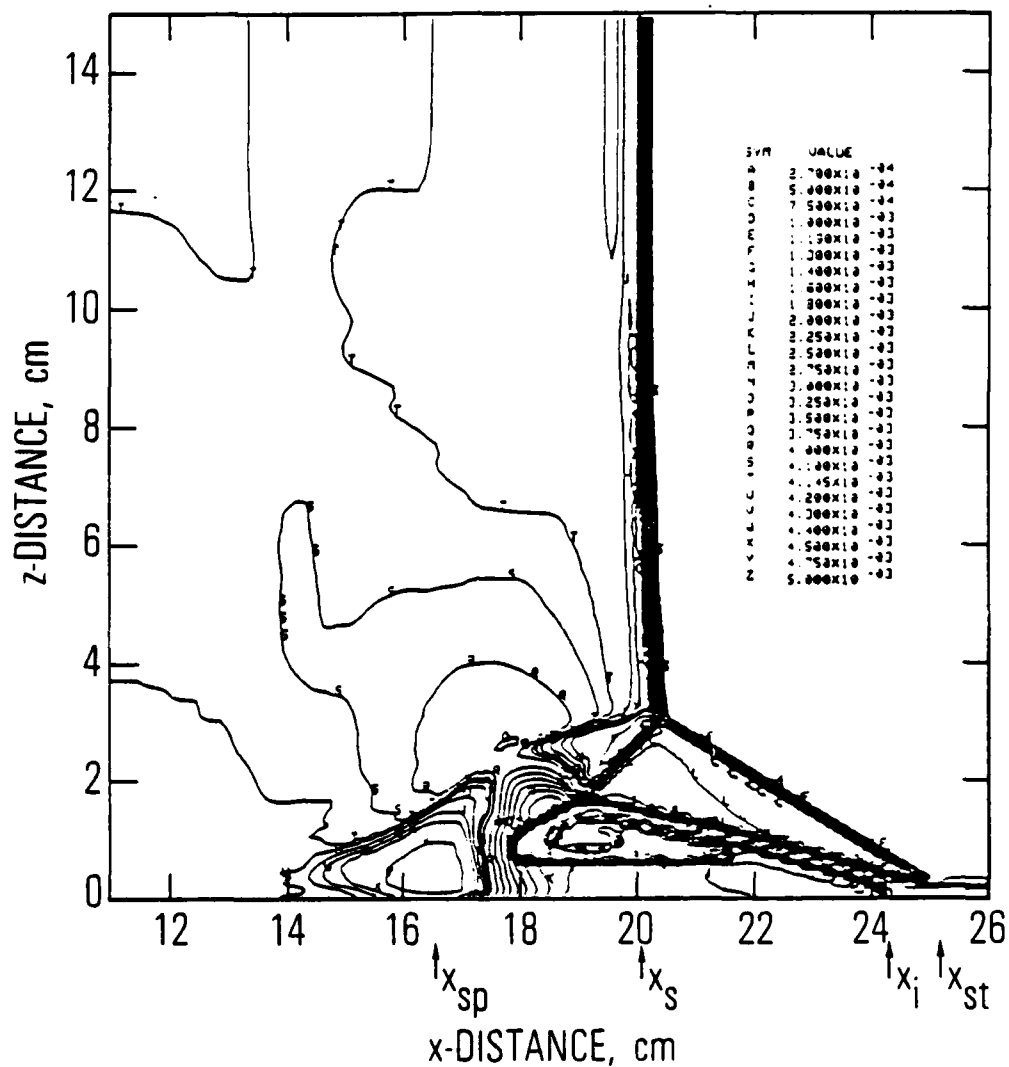


Fig. 4a. Numerical Results of Ref. 5 for Shock-Thermal Layer Interaction. Case II, $x_s = 20.1$ cm. Initial conditions noted in Table 1. (Contours of constant density, overall).

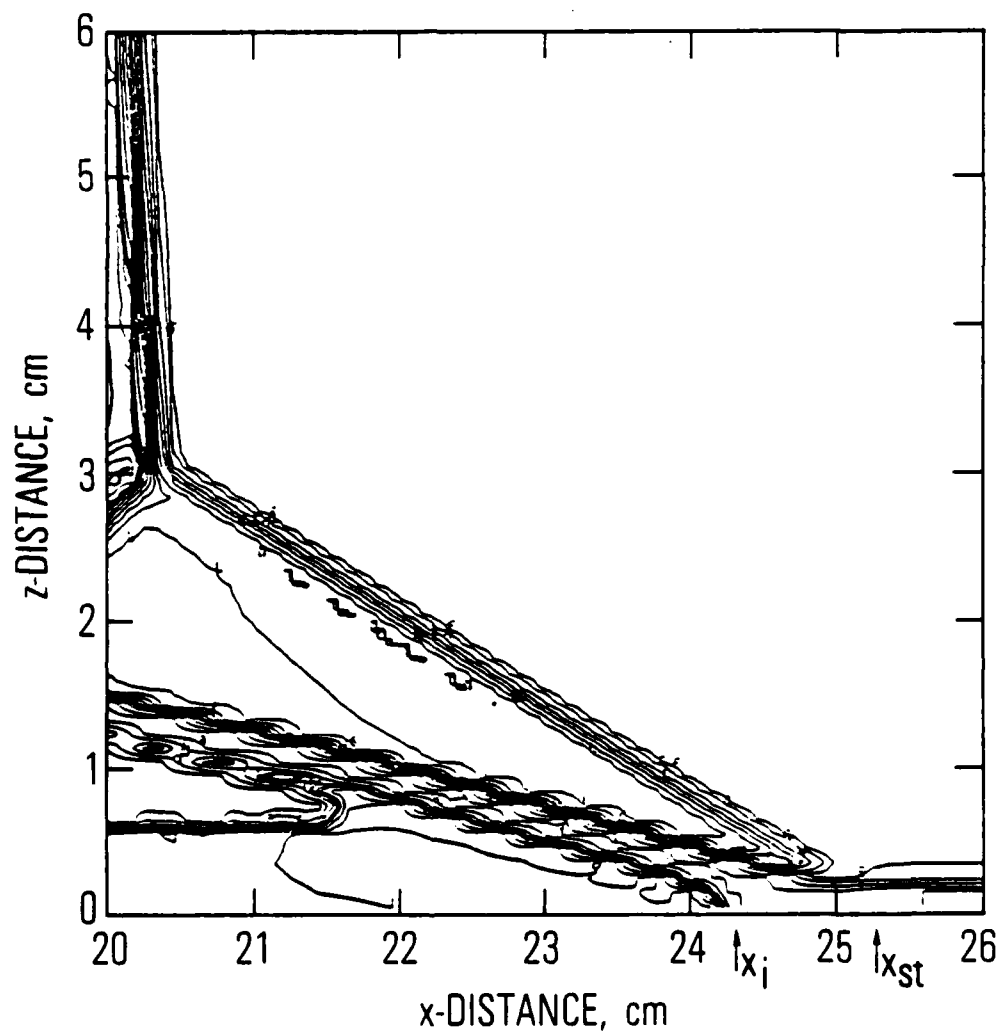


Fig. 4b. Numerical Results of Ref. 5 for Shock-Thermal Layer Interaction. Case II, $x_s = 20.1$ cm. Initial conditions noted in Table 1. (Contours of constant density, detail).

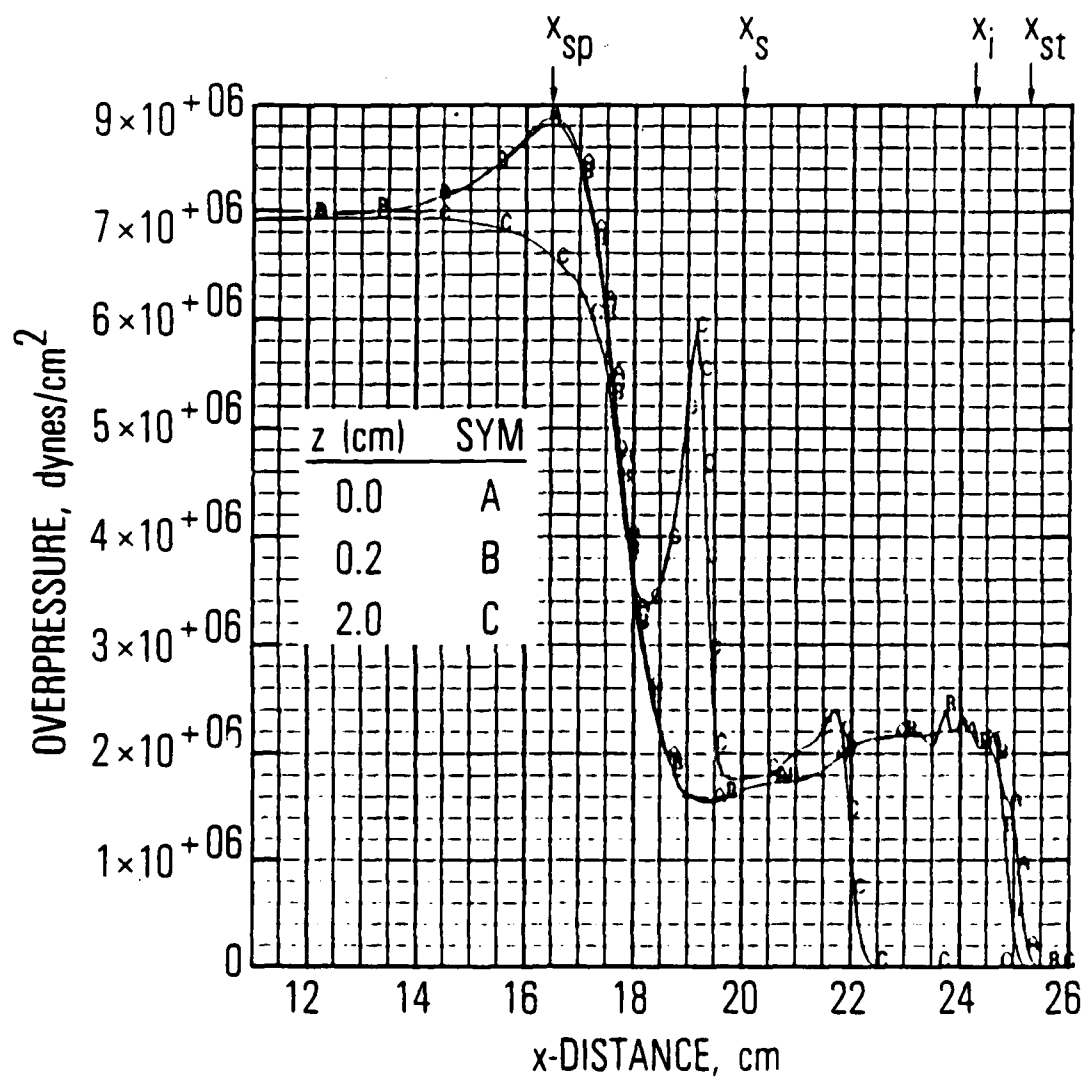


Fig. 4c. Numerical Results of Ref. 5 for Shock-Thermal Layer Interaction. Case II, $x_s = 20.1$ cm. Initial conditions noted in Table 1. (Overpressure at three heights ($p_1 = 1.013 \times 10^6$ dynes/cm²)).

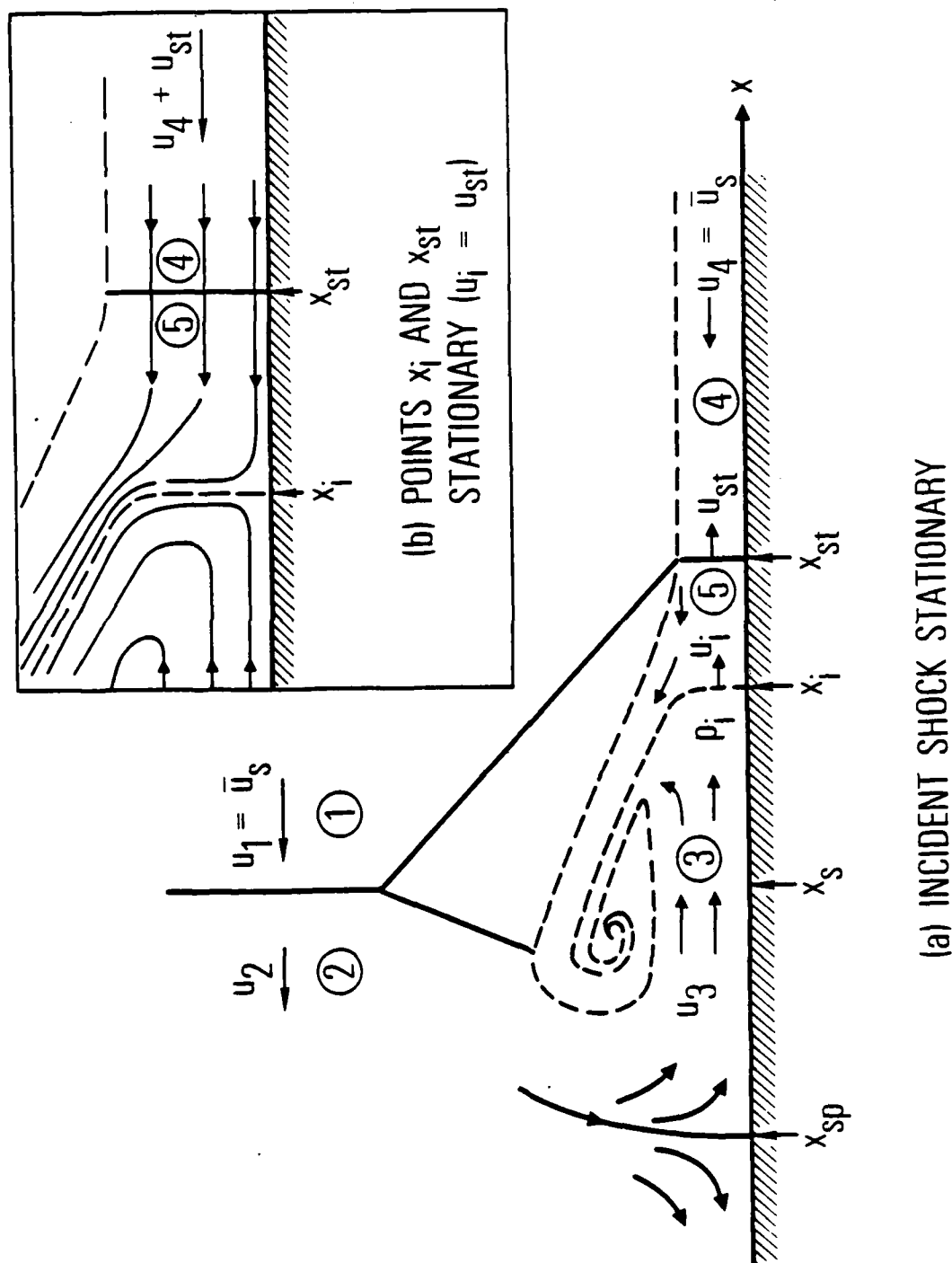


Fig. 5. Schematic Representation of Shock-Thermal Layer Interaction for Case of Separated Flow

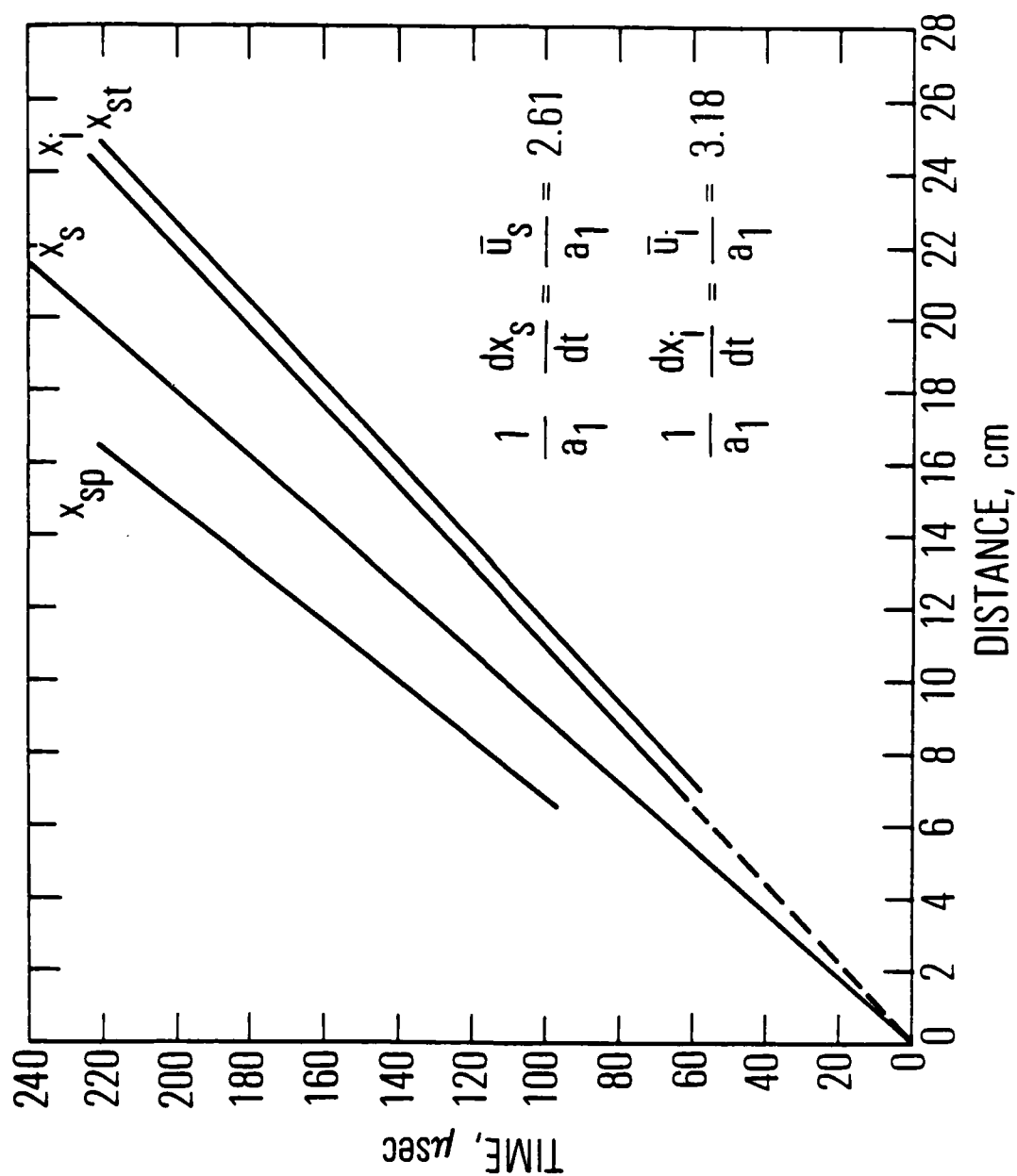


Fig. 6a. Interface Trajectories Based on Numerical Solution of Ref. 5. Initial conditions noted in Table 1. (Case II ($a_4/a_1 = 2.26$, $\bar{M}_8 = 2.61$)).

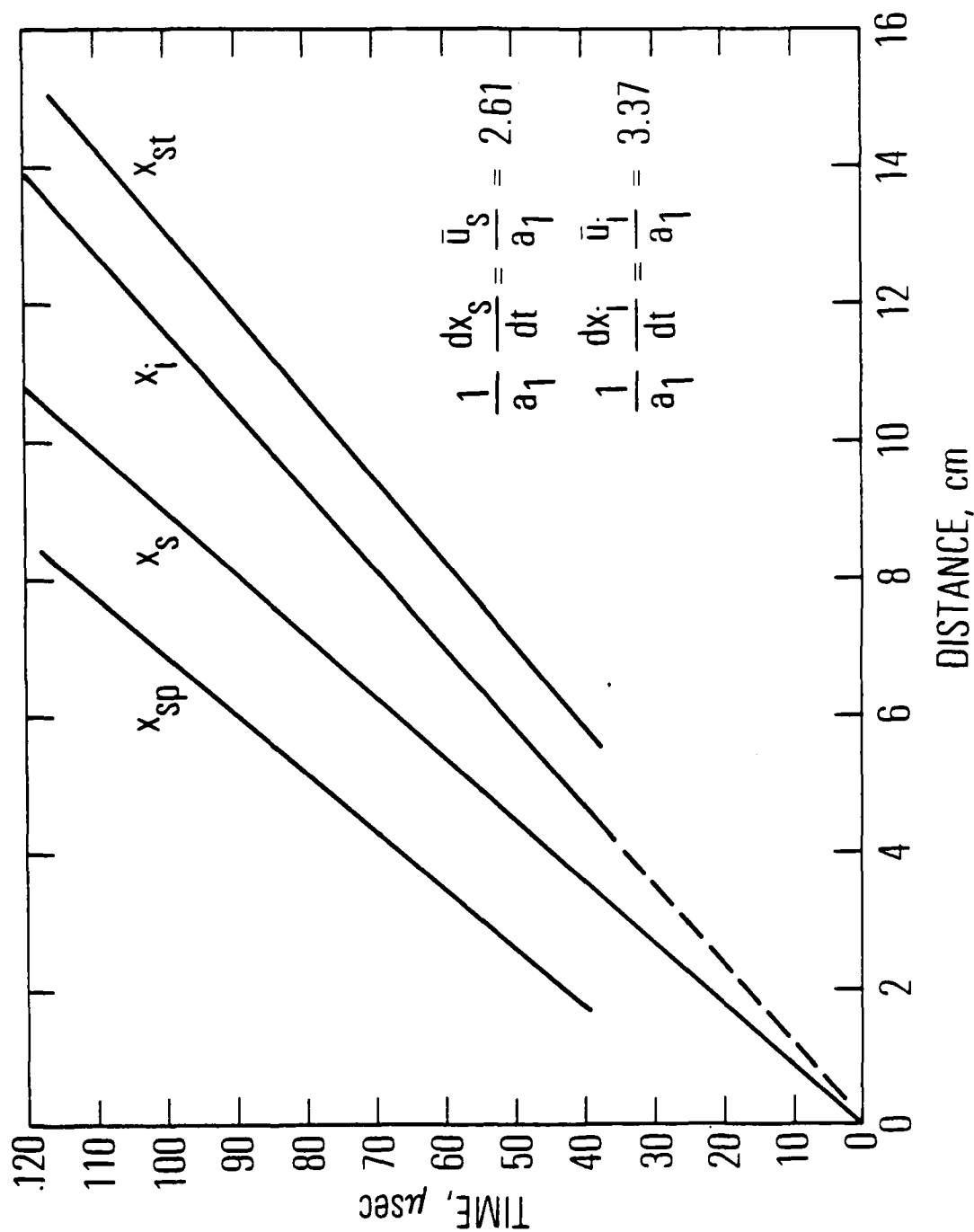


Fig. 6b. Interface Trajectories Based on Numerical Solution of Ref. 5. Initial conditions noted in Table I. (Case VII ($a_4 a_1 = 2.92$, $\bar{M}_s = 2.61$)).

Table 1. Comparison of Numerical Results of Ref. 5 with Present Analytic Model. Initial

conditions are $\gamma_1 = 1.4$, $\gamma_4 = 5/3$, $T_1 = 293$ K, $a_1 = 3.46 \times 10^4$ cm/sec,
 $p_1 = 1.013 \times 10^6$ dynes/cm², $h = 0.2$ cm, $p_2/p_1 = 7.80$, $\bar{M}_s = 2.61$.

Case	\bar{M}_s	a_4/a_1	x_s , cm	u_1/a_1	\bar{M}_{st}	p_{sp}/p_1	p_1/p_1	$(p_1/p_1)\bar{M}_{st}^b$
II (Ref. 5)	2.61	2.26	8.8	0.57	1.41	8.0	3.2	3.4
			13.7	0.57	1.41	8.3	3.2	3.4
			20.1	0.57	1.41	8.7	3.2	3.4
$k = 0.27^a$				0.47	1.36	9.2	3.2	
$k = 1.00^a$				1.37	1.76	9.2	5.0	
VII (Ref. 5)	2.61	2.92	3.4	0.76	1.15	7.7	2.6	2.5
			7.0	0.76	1.15	7.9	2.6	2.5
			10.5	0.76	1.15	8.3	2.6	2.5
$k = 0.27^a$				0.53	1.08	9.2	2.3	
$k = 1.00^a$				1.66	1.41	9.2	3.7	

^aAnalytic model

^b p_1/p_1 computed from \bar{M}_{st} and Eq. 6(a)

interface location x_i moves with constant speed. The wall stagnation point location x_{sp} moves with a velocity approximately equal to that of the incident shock x_s and, hence, is stationary in incident shock coordinates. Similarly, the leading edge of the normal shock in the thermal layer x_{st} moves with approximately the same velocity as x_i . Thus, the separation distance $x_{st} - x_i$ remains constant. The flow in a coordinate system wherein x_{st} and x_i are stationary is illustrated in Fig. 5(b). The flow in region 5 is steady in this coordinate system. These results suggest an analytic model described in the next section.

2. ANALYTIC MODEL

We consider the flow in an incident shock stationary coordinate system as shown in Fig. 5(a). The stagnation point x_{sp} is assumed to be stationary, and the separation distance $x_{st} - x_i$ is assumed to remain constant for cases when a shock develops in the thermal layer. Flow conditions in each of the regions noted in Fig. 5 are obtained from the following expressions.

a. Region 2

Region 2 is the uniform region downstream of the incident shock. Normal shock relations indicate⁶

$$\frac{p_2}{p_1} = \frac{2\gamma_1 M_1^2 - (\gamma_1 - 1)}{\gamma_1 + 1} \quad (3a)$$

$$\frac{p_{2,t}}{p_1} = \left[\frac{(\gamma_1 + 1)M_1^2}{2} \right]^{\gamma_1/(\gamma_1 - 1)} \left[\frac{\gamma_1 + 1}{2\gamma_1 M_1^2 - (\gamma_1 - 1)} \right]^{1/(\gamma_1 - 1)} \quad (3b)$$

where $p_{2,t}$ is the stagnation pressure in region 2. Since x_{sp} is stationary in the present coordinate system,

$$p_{sp}/p_1 = p_{2,t}/p_1 \quad (3c)$$

The possibility that the flow at p_{sp} was processed by the oblique-normal shock structure at the base of the incident shock is ignored in Eq. 3(c). However, the effect on p_{sp} should not be large.

b. Region 3

Conditions in region 3 are assumed to result from a steady isentropic expansion from conditions in region 2. Expressions of interest are

$$\frac{p_3}{p_1} \equiv \frac{p_3}{p_{3,t}} \frac{p_{2,t}}{p_1} = \left[1 + \frac{(\gamma_1 - 1)M_3^2}{2} \right]^{-\gamma_1/(\gamma_1 - 1)} \frac{p_{2,t}}{p_1} \quad (4a)$$

$$\frac{u_3}{a_1} \equiv \frac{u_3}{a_3} \frac{a_3/a_{3,t}}{a_1/a_{1,t}} = M_3 \left[\frac{2 + (\gamma_1 - 1)M_3^2}{2 + (\gamma_1 - 1)M_1^2} \right]^{-1/2} \quad (4b)$$

$$\begin{aligned} \frac{\bar{Q}_3}{\bar{Q}_2} &\equiv \frac{\rho_3(\bar{u}_3)^2}{\rho_2(\bar{u}_2)^2} \\ &= \left[\frac{2 + (\gamma_1 - 1)M_3^2}{2 + (\gamma_1 - 1)M_2^2} \right]^{-1/(\gamma_1 - 1)} \left[\frac{(u_3/a_1) + M_1}{2(\gamma_1 + 1)^{-1}(M_1 - M_1^{-1})} \right]^2 \end{aligned} \quad (4c)$$

where \bar{Q} denotes dynamic pressure in laboratory coordinates.

c. Region 5

For cases in which a shock develops in the thermal layer, the separation distance $x_{st} - x_i$ is assumed to remain constant (Fig. 6). The flow in region 5 is then equivalent to steady supersonic flow with Mach number

$$\bar{M}_{st} \equiv \frac{\bar{u}_{st}}{a_4} = \frac{\bar{u}_i}{a_4} = \frac{M_1 + (u_i/a_1)}{a_4/a_1} \quad (5)$$

over a blunt body defined by the interface at x_1 . For cases in which a shock does not develop, the flow in region 5 is equivalent to subsonic flow at Mach number \bar{u}_1/a_4 over a blunt body defined by the interface. The pressure p_1 corresponds to the stagnation pressure at the nose of the equivalent body and is found from

$$\frac{p_1}{p_1} = \left[\frac{(\gamma_4 + 1) \bar{M}_{st}^2}{2} \right]^{\gamma_4/(\gamma_4 - 1)} \left[\frac{\gamma_4 + 1}{2\gamma_4 \bar{M}_{st}^2 - (\gamma_4 - 1)} \right]^{1/(\gamma_4 - 1)} \quad \bar{M}_{st} > 1 \quad (6a)$$

$$= \left[1 + \frac{\gamma_4 - 1}{2} \left(\frac{\bar{u}_1}{a_4} \right)^2 \right]^{\gamma_4/(\gamma_4 - 1)} \quad \bar{u}_1/a_4 < 1 \quad (6b)$$

where \bar{M}_{st} and \bar{u}_1/a_4 can be used interchangeably (Eq. 5).

d. Method of Solution

The interaction is uniquely determined by specification of the initial conditions \bar{M}_s , γ_1 , γ_4 , a_4/a_1 , and h . (The quantity h is not needed, however, for the present model.) Estimates for flow properties can be obtained from the previous equations if the boundary conditions at the interface location x_1 are specified. In the present model, we assume that conditions in regions 3 and 5, at x_1 , are related by

$$p_1 = p_3 \quad (7a)$$

$$u_1 = k u_3 \quad (7b)$$

The arbitrary constant k is introduced to permit matching of the analytic model with numerical code calculations. A value of $k < 1$ can be interpreted as indicating a transverse velocity in region 3 at the interface (Fig. 7). A simple procedure for evaluating the previous equations is to specify γ_1 , γ_4 , $M_1 \equiv \bar{M}_s$, and M_3 . \bar{M}_{st} (or, equivalent, \bar{u}_1/a_4) is found, by iteration, by

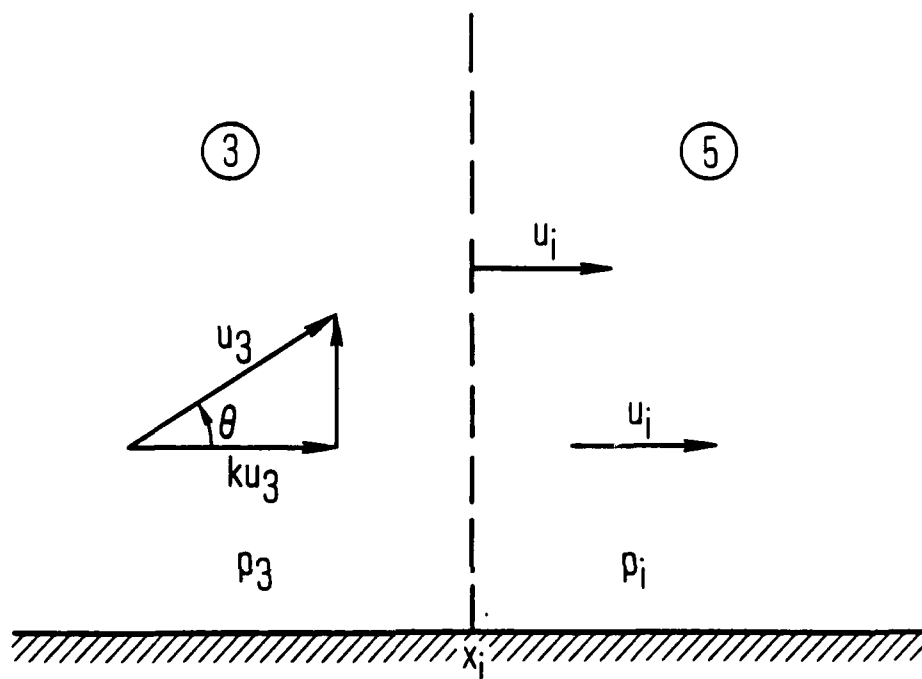


Fig. 7. Boundary Conditions Near Interface x_i in Incident Shock Stationary Coordinate System, $k \equiv \cos \theta$.

equating Eqs. 6 and 4(a). The corresponding values of a_4/a_1 and \bar{u}_1/a_1 are obtained from Eqs. 5 and 7(b), namely

$$a_4/a_1 = [(M_1 + (ku_3/a_1))/\bar{M}_{st}] \quad (8a)$$

$$\bar{u}_1/a_1 = (\bar{u}_1/a_4)(a_4/a_1) \quad (8b)$$

Using the present procedure, a_4/a_1 and \bar{u}_1/a_1 are the only quantities that depend on the value of k . Numerical results are given in Table 2 for the case $k = 1$. For a given incident shock \bar{M}_s , the dynamic pressure ratio \bar{Q}_3/\bar{Q}_2 has a maximum at a particular value of a_4/a_1 . The maximum is characteristic of the isentropic expansion to M_3 . Values of \bar{M}_{st} in the range $\bar{M}_{st} < 1$ indicate that a shock is not formed in the thermal layer.

Table 2. Results of Analytical Model for $k = 1$, $\gamma_1 = 1.4$, and $\gamma_4 = 1.4$, $5/3$

\bar{M}_8	M_3	u_3/a_1	p_3/p_1	$\gamma_4 = 1.4$				$\gamma_4 = 5/3$			
				a_4/a_1	\bar{M}_{st}	Q_3/Q_2	a_4/a_1	\bar{M}_{st}	Q_3/Q_2	a_4/a_1	\bar{M}_{st}
1.100	1.100	1.017	1.127	1.963	.880	148.668	2.103	.828	148.668	2.103	.828
1.100	.900	.839	1.393	2.733	.710	161.543	2.955	.657	161.543	2.955	.657
1.100	.700	1.017	1.127	5.005	.416	164.943	5.529	.383	164.943	5.529	.383
1.500	.400	.774	3.057	1.406	1.402	9.443	1.501	1.316	9.443	1.501	1.316
1.500	.300	.693	2.670	1.706	1.288	10.642	1.818	1.209	10.642	1.818	1.209
1.500	.200	.907	1.393	2.111	1.140	11.239	2.252	1.063	11.239	2.252	1.063
1.500	.100	1.017	1.127	3.812	.958	11.446	3.911	.893	11.446	3.911	.893
1.500	1.400	1.429	1.077	9.211	.318	9.836	10.023	.292	9.836	10.023	.292
2.000	.200	.267	5.495	1.151	1.965	3.790	1.223	1.877	3.790	1.223	1.877
2.000	.100	.527	5.052	1.444	1.881	4.436	1.463	1.754	4.436	1.463	1.754
2.000	.000	.774	3.057	1.591	1.574	5.048	1.693	1.637	5.048	1.693	1.637
2.000	.000	1.017	1.127	2.312	1.380	5.668	2.311	1.439	5.668	2.311	1.439
2.000	1.200	1.492	1.172	3.811	1.173	7.245	4.112	1.279	7.245	4.112	1.279
3.000	.200	.299	9.202	1.136	2.357	5.074	1.203	2.310	5.074	1.203	2.310
3.000	.100	.540	8.594	1.311	2.357	5.429	1.393	2.107	5.429	1.393	2.107
3.000	.000	.774	5.549	1.583	2.194	6.123	1.634	1.857	6.123	1.634	1.857
3.000	.000	1.017	3.313	2.303	1.767	6.974	2.335	1.654	6.974	2.335	1.654
3.000	1.200	1.460	1.172	3.812	1.529	8.974	4.339	1.421	8.974	4.339	1.421
4.000	.200	.299	7.902	1.129	2.957	4.695	1.203	2.775	4.695	1.203	2.775
4.000	.100	.540	7.412	1.305	2.842	5.257	1.393	2.554	5.257	1.393	2.554
4.000	.000	.774	5.549	1.577	2.686	6.033	1.634	2.393	6.033	1.634	2.393
4.000	.000	1.017	3.313	2.303	2.369	7.459	2.335	2.179	7.459	2.335	2.179
4.000	1.200	1.460	1.172	3.812	2.194	9.745	4.339	1.949	9.745	4.339	1.949
5.000	.200	.299	11.000	1.129	3.957	4.995	1.203	3.654	4.995	1.203	3.654
5.000	.100	.540	10.412	1.305	3.842	5.557	1.393	3.434	5.557	1.393	3.434
5.000	.000	.774	7.902	1.577	3.686	6.333	1.634	3.273	6.333	1.634	3.273
5.000	.000	1.017	5.549	2.303	3.369	7.759	2.335	3.063	7.759	2.335	3.063
5.000	1.200	1.460	1.172	3.812	3.194	9.974	4.339	2.799	9.974	4.339	2.799
6.000	.200	.299	12.900	1.129	4.057	4.995	1.203	3.654	4.995	1.203	3.654
6.000	.100	.540	12.412	1.305	3.942	5.557	1.393	3.434	5.557	1.393	3.434
6.000	.000	.774	10.412	1.577	3.786	6.333	1.634	3.273	6.333	1.634	3.273
6.000	.000	1.017	7.902	2.303	3.469	7.759	2.335	3.063	7.759	2.335	3.063
6.000	1.200	1.460	1.172	3.812	3.294	9.974	4.339	2.799	9.974	4.339	2.799
7.000	.200	.299	14.900	1.129	4.157	4.995	1.203	3.654	4.995	1.203	3.654
7.000	.100	.540	14.412	1.305	4.042	5.557	1.393	3.434	5.557	1.393	3.434
7.000	.000	.774	12.412	1.577	3.886	6.333	1.634	3.273	6.333	1.634	3.273
7.000	.000	1.017	10.412	2.303	3.569	7.759	2.335	3.063	7.759	2.335	3.063
7.000	1.200	1.460	1.172	3.812	3.394	9.974	4.339	2.799	9.974	4.339	2.799

III. DISCUSSION

The present analytic model is compared in Table 1 with numerical data from Ref. 5. Values of u_1/a_1 , \bar{M}_{st} , p_{sp}/p_1 , and p_i/p_1 , from Ref. 5, are given as a function of incident shock location x_s for two initial conditions (Cases II and VII). Analytic estimates for these quantities, based on $k = 1.00$ and $k = 0.27$, are included in Table 1. The values of p_{sp}/p_1 in Ref. 5 increase with x_s and appear to approach the analytic estimate. Hence, the assumption $p_{sp}/p_1 = p_{2,t}/p_1$ [Eq. 3(c)] appears reasonable. Other analytic estimates in Table 1 depend on the choice for k . The initial choice, $k = 1.00$, led to an overestimate of u_1/a_1 , \bar{M}_{st} , and p_i/p_1 . However, the variation of these quantities with a_4/a_1 had the proper trend. The second value, $k = 0.27$, was chosen so that the analytic estimate for p_i/p_1 would agree with the numerical result in Ref. 5 for Case II. This led to improved correlations between the analytic model and the Cases II and VII data from Ref. 5. However, the usefulness of the approximation $k = 0.27$ for other initial conditions is uncertain and requires further study.

The interface pressure p_i/p_1 was also computed from Eq. 6(a) using the value of \bar{M}_{st} deduced from the data in Ref. 5. The resulting pressure is denoted $(p_i/p_1)_{\bar{M}_{st}}$ in Table 1 and agrees with the value of p_i/p_1 reported in Ref. 5. This calculation confirms the analytic model assumption that the pressure p_i/p_1 equals the stagnation pressure associated with \bar{M}_{st} (Eq. 6).

IV. CONCLUSION

Numerical solutions⁵ for the inviscid interaction between a moving shock and a thermal layer have been reviewed. The streamwise locations x_{sp} , x_s , x_i , and x_{st} were of particular interest. It was determined that after an initial transient $dx_{sp}/dt \doteq dx_s/dt \equiv \bar{u}_s$. This led to the assumption, in the analytic model, that the pressure at x_{sp} can be equated to the stagnation pressure behind the incident shock in incident shock stationary coordinates ($p_{sp} = p_{2,t}$). Similarly, it was concluded that after an initial transient $dx_{st}/dt \doteq dx_i/dt \equiv \bar{u}_i$. Hence, the pressure p_i at x_i was assumed, in the analytic model, to be equivalent to the stagnation pressure on a blunt body in a Mach number $\bar{M}_{st} = \bar{u}_i/a_4$ flow. The analytic model was only partly successful in predicting x_i and p_i . The introduction of a free constant $k = u_3/u_1$ was required. This constant is related to the angularity of the flow in region 3. The choice $k = 0.27$ led to good agreement between the analytic model and data from cases II and VII. However, the large departure of k , from one, makes the physical interpretation questionable. Further comparisons with numerical solutions are needed to validate the analytic model.

In the present inviscid model, the scale of the disturbed flow grows linearly and without limit. It is expected that viscous effects will cause the flow to approach an asymptotic limit. The scale and nature of the flow, in this limit, also requires further study.

REFERENCES

1. Glasstone, S. and Dolan, P. J., "The Effects of Nuclear Weapons," U.S. Government Printing Office, Washington, D.C., 1977, p. 125.
2. Hess, R. V., "Interaction of Moving Shocks and Hot Layers," NACA TN 4002, 1957.
3. Griffith, W. C., "Interaction of a Shock Wave with a Thermal Boundary Layer," Jour. Aero. Sci., Jan. 1956.
4. Gion, E. J., "Plane Shock Interacting with Thermal Layer," Physics of Fluids, Vol. 20, No. 4, April 1977.
5. Schneyer, G. P., and Wilkins, D. E., "Thermal Layer-Shock Interaction (Precursor) Simulation Data Book," S-Cubed Report No. SSS-R-84-6584, Mar. 1984.
6. Ames Research Staff, "Equations, Tables and Charts for Compressible Flow," NACA TR 1135, 1953.

SYMBOLS

a	speed of sound
h	initial height of thermal layer
k	arbitrary constant, $k < 1$
M	Mach number in incident shock stationary coordinate system, u/a
\bar{M}	Mach number in laboratory coordinates, \bar{u}/a
p	pressure
\bar{Q}	dynamic pressure in laboratory coordinates, $\rho(\bar{u})^2/2$
t	time
u, \bar{u}	velocity
x, z	streamwise and vertical directions, respectively
γ	ratio of specific heats

SUBSCRIPTS

$1, 2, 3, 4, 5$	flow regions
i	interface value
s	incident shock
st	shock in thermal layer
sp	stagnation point at foot of incident shock
t	stagnation value

SUPERSCRIPTS

$(\bar{\quad})$	superscript bar denotes laboratory coordinates
(\quad)	absence of superscript bar denotes incident shock stationary coordinates

LABORATORY OPERATIONS

The Aerospace Corporation functions as an "architect-engineer" for national security projects, specializing in advanced military space systems. Providing research support, the corporation's Laboratory Operations conducts experimental and theoretical investigations that focus on the application of scientific and technical advances to such systems. Vital to the success of these investigations is the technical staff's wide-ranging expertise and its ability to stay current with new developments. This expertise is enhanced by a research program aimed at dealing with the many problems associated with rapidly evolving space systems. Contributing their capabilities to the research effort are these individual laboratories:

Aerophysics Laboratory: Launch vehicle and reentry fluid mechanics, heat transfer and flight dynamics; chemical and electric propulsion, propellant chemistry, chemical dynamics, environmental chemistry, trace detection; spacecraft structural mechanics, contamination, thermal and structural control; high temperature thermomechanics, gas kinetics and radiation; cw and pulsed chemical and excimer laser development including chemical kinetics, spectroscopy, optical resonators, beam control, atmospheric propagation, laser effects and countermeasures.

Chemistry and Physics Laboratory: Atmospheric chemical reactions, atmospheric optics, light scattering, state-specific chemical reactions and radiative signatures of missile plumes, sensor out-of-field-of-view rejection, applied laser spectroscopy, laser chemistry, laser optoelectronics, solar cell physics, battery electrochemistry, space vacuum and radiation effects on materials, lubrication and surface phenomena, thermionic emission, photo-sensitive materials and infrared detectors, atomic frequency standards, and environmental chemistry.

Computer Science Laboratory: Program verification, program translation, performance-sensitive system design, distributed architectures for spaceborne computers, fault-tolerant computer systems, artificial intelligence, microelectronics applications, communication protocols, and computer security.

Electronics Research Laboratory: Microelectronics, solid-state device physics, compound semiconductors, radiation hardening; electro-optics, quantum electronics, solid-state lasers, optical propagation and communications; microwave semiconductor devices, microwave/millimeter wave measurements, diagnostics and radiometry, microwave/millimeter wave thermionic devices; atomic time and frequency standards; antennas, RF systems, electromagnetic propagation phenomena, space communication systems.

Materials Sciences Laboratory: Development of new materials: metals, alloys, ceramics, polymers and their composites, and new forms of carbon; non-destructive evaluation, component failure analysis and reliability; fracture mechanics and stress corrosion; analysis and evaluation of materials at cryogenic and elevated temperatures as well as in space and enemy-induced environments.

Space Sciences Laboratory: Magnetospheric, auroral and cosmic ray physics, wave-particle interactions, magnetospheric plasma waves; atmospheric and ionospheric physics, density and composition of the upper atmosphere, remote sensing using atmospheric radiation; solar physics, infrared astronomy, infrared signature analysis; effects of solar activity, magnetic storms and nuclear explosions on the earth's atmosphere, ionosphere and magnetosphere; effects of electromagnetic and particulate radiations on space systems; space instrumentation.

END

DTIC

4-86